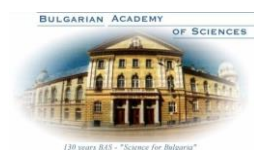


FOURTEENTH WORKSHOP
**Solar Influences on the Magnetosphere,
Ionosphere and Atmosphere**

Primorsko, Bulgaria, June 06÷10, 2022



SPACE RESEARCH AND TECHNOLOGY INSTITUTE
BULGARIAN ACADEMY of SCIENCES



Scientific Organizing Committee

Katya Georgieva (Space Research and Technology Institute, Sofia, Bulgaria) – *Chair*
Atila Özgüç (Bogazici Univ. Kandilli Observatory, Istanbul, Turkey)
Crisan Demetrescu (Institute of Geodynamics, Romanian Academy)
Dragan Roša (Zagreb Astronomical Observatory, Croatia)
Jean-Pierre Rozelot (Université Côte d'Azur)
Nat Gopalswamy (NASA Goddard Space Flight Center)
Olga Malandraki (IAASARS, National Observatory of Athens, Greece)
Petra Koucká Knížová (Institute of Atmospheric Physics, Czech Republic)
Vladimir Obridko (IZMIRAN, Moscow, Russian Federation)

Topics:

Sun and Solar Activity
Solar Wind-Magnetosphere-Ionosphere Interactions
Solar Influences on the Lower Atmosphere and Climate
Solar Effects in the Biosphere and Lithosphere
Instrumentation for Space Weather Monitoring
Data Processing and Modelling

Local Organizing Committee:

(Space Research and Technology Institute, Sofia, Bulgaria):

Boian Kirov – *Chair*;
Simeon Asenovski;
Kostadinka Koleva.



The 14th workshop is supported by
the Bulgarian National Science Fund,
Grant No KP-06-MNF/2,
SCOSTEP/PRESTO program,
and Bulgarian Academy of Sciences.



DOI: 10.31401/WSoz.2022.abs

CONTENTS

Sun and Solar Activity

<i>Calisir M.A., Kilcik A.</i> Relationship between Solar Energetic Particles and Solar Flares during the 24th Solar Cycle	01
<i>Dechev M., Koleva K., Duchlev P., Simic Z., Chandra R.</i> Different Prominence Eruptions and Associated Coronal Mass Ejections	01
<i>Demiroz M.I., Kilcik A.</i> Coronal Mass Ejection Effect on Interplanetary Medium: A Case Study	01
<i>Isaeva E.</i> Diagnostics of Solar Proton Events Based on the Parameters of Type II and IV Radio Bursts	02
<i>Katsova M., Nizamov B., Shlyapnikov A.</i> Activity of Solar Twins	02
<i>Kirov B., Georgieva K., Asenovski S.</i> A Comparison Between the Solar Activity in the 11-Year Sunspot Cycles During the Last Two Centennial Solar Activity Minima. A Comparison of the Geomagnetic Activity During the Same Periods	03
<i>Kobyliński Z., Wysokiński A.</i> Forecast of the Solar and Geomagnetic Activity During 25 - 26 Cycles by Means of Elman ANN	03
<i>Koleva K., Dechev M., Duchlev P., Chandra R.</i> Solar Asymmetric Filament Eruption Observed by the Solar Dynamic Observatory and Related Activity	04
<i>Kolotkov D.Y.</i> Hidden Timescales in Solar and Stellar Flares	04
<i>Kostov M.</i> Structure of the Solar Corona During the Solar Cycle Rising Phase	05
<i>Krastev K., Semkova J., Koleva R., Benghin V., Drobijshv S.</i> Solar Manifestations in the Martian Orbit Observed from the Liulin Instrument	05
<i>Malandraki O.E., Rodríguez-Pacheco J., McComas D.J., Wimmer-Schweingruber R.F., Schwadron N., Ho G.C., Desai M., Mitchel D.G., Kollhoff A., Janitzek N., Pacheco D., Gomez-Herrero R., Posner A., Kouloumvakos A., Dresing N., Heber B., Cohen C.M.S., Kuehl P., Leske R., Wiedenbeck M. and the Solar Orbiter/EPD and PSP/ISOIS teams.</i> Pioneering Energetic Particle Observations Near the Sun by Solar Orbiter and Parker Solar Probe	06
<i>Muraközy J.</i> Variations of the Sunspot Groups Separation Distance and Tilt Angles During the Decay	07
<i>Obridko V.N., Katsova M.M., Sokoloff D.D., Shelting B.D., Livshits I.M.</i> Clarifying Physical Properties of Magnetic Fields in Sunspots	07
<i>Ozguc A., Kilcik A., Yurchyshyn V.</i> Temporal and Periodic Variations of the Solar Flare Index during Last Four Solar Cycles and their Association with Selected Interplanetary Parameters	08
<i>Podgorny A.I., Podgorny I.M., Borisenko A.V.</i> Singularities of the Magnetic Field Configuration During Flares M1.4 on May 27, 2003 at 02:43 and M 1.9 on May 26, 2003 at 05:34 According to the Results of MHD Simulation Above the Active Region AR 10365	08
<i>Semkova J., Koleva R., Benghin V., Krastev K., Matviichuk Y., Tomov B., Bankov N., Maltchev S., Dachev T., Mitrofanov I., Malakhov A., Kozyrev A., Golovin D., Mokrousov M., Sanin A., Litvak M., Nikiforov S., Lisov D., Anikin A., Shurshakov V., Drobyshev S.</i> Observation of Solar Energetic Particle Events Onboard ExoMars TGO in July 2021-March 2022	09

<i>Sokoloff D., Malova Y., Maiewsky E., Yushkov E., Popov V.</i> Stellar Dynamo and Structure of Current Sheets	09
<i>Tsvetkov Ts., Nakeva Y., Petrov N.</i> Database of Solar Cycle 24 Coronal Mass Ejections and Flares Related to Active Regions	09
<i>Yermolaev Y.I., Lodkina I.G., Khokhlachev A.A., Yermolaev M.Yu., Riazantseva M.O., Rakhmanova L.S., Borodkova N.L., Sapunova O.V., Moskaleva I A.V.</i> Possible Causes and Consequences of the Weakening of the Solar Wind in the Current Epoch of the Grand Solar Minimum	10
<i>Zhukova A., Khlystova A., Abramenko V., Sokoloff D.</i> Temporal and Latitudinal Distribution of Anti-Hale Active Regions in the Synthetic Solar Cycle	10
Solar Wind-Magnetosphere-Ionosphere Interactions	
<i>Demetrescu C., Dobrica V., Stefan C.</i> Toward the Space Climate Characterization of the Heliosphere – Magnetosphere Environment for the Last 400 Years	11
<i>Despirak I.V., Werner R., Lubchich A.A., Kleimenova N.G., Guineva V.</i> Relationship Between the Intense Mid-Latitude Geomagnetic Effect at the Panagurishte Station and Solar Wind Conditions	11
<i>Despirak I.V., Lubchich A.A., Kleimenova N.G., Setsko P.V., Werner R.</i> Supersubstorm on 20 December 2015: Spatial Geomagnetic Effects	12
<i>Feygin F. Z., Khabazin Yu. G., Kleimenova N. G., Malysheva L. M.</i> Ground-based Pc1 geomagnetic pulsation polarization as a proxy of the plasmopause location	12
<i>Gopalswamy N., Yashiro S., Xie H., Akiyama S., Mäkelä P.</i> Effect of Solar Wind Density in the Time Structure of Geomagnetic Storms	13
<i>Gromova L.I., Kleimenova N.G., Despirak I.V., Lubchich A.A., Gromov S.V., Malysheva L.M.</i> Polar Geomagnetic Disturbances and Auroral Substorms During the Magnetic Storm on 20 April 2020	13
<i>Guineva V., Werner R., Bojilova R., Atanassov A., Raykova L., Valev D.</i> Maps of the Spatial Distribution of the Variations in the X and Y Components of the Magnetic Field at European Midlatitudes During Substorms: A Case Study	14
<i>Jivov I., Bojilova R.</i> Comparison of Ionospheric and Geomagnetic Anomalies over Bulgaria during St. Patrick's Geomagnetic Storm	14
<i>Kilcik A., Tirnakci M.</i> Comparison of the Critical Frequencies of the Ionospheric F1 and F2 Layers with the X-Ray Solar Flare Numbers Observed during the Solar Cycle 24	15
<i>Kirov B., Georgieva K.</i> Solar Magnetic Field and Earth Rotation	15
<i>Kleimenova N.G., Despirak I.V., Malysheva L.M., Gromova L.I., Lubchich A.A., Guineva V., Werner R.</i> Morning Polar Substorms and Their Possible Mid-Latitude Effects	16
<i>Koucká Knížová P., Podolská K., Mošna Z., Kouba D., Potužníková K.</i> Ionospheric Variability Observed During 4 November 2021 Geomagnetic Storm	16
<i>Setsko P.V., Despirak I.V., Sakharov Ya.A., Bilin V.A., Selivanov V.N.</i> Appearance of GICs in Case of Two SuperSubStorms on September 7 and 8, 2017	17
<i>Stefan C., V. Dobrica V., Demetrescu C.</i> Assessing the Possible Sources of the Geomagnetic Storms By Means of Empirical Orthogonal Function Analysis	17
<i>Werner R., Guineva V., Atanassov A., Bojilova R., Raykova L., Valev D., Despirak I.V., Lubchich A.A., Kleimenova N.G., Setsko P.V.</i> Mid-Latitude Response to Auroral Substorms in Magnetic Field Variations at the Bulgarian Station Panagjurishte from 2007 Up to 2020	18

Data Processing and Modelling

<i>Adibekyan M.</i> Analyse of Ionospheric and Geomagnetic Pre -Earthquake Anomalies	19
<i>Asenovski S., Georgieva K., Kirov B.</i> Open Access Database for Different Types of Solar Wind	19
<i>Bojilova R., Mukhtarov P.</i> The Methodology for Calculating the Values of Monthly Median Critical Frequencies of E-Region	19
<i>Dineva E., Denker C., Verma M., Steffen M., Kontogiannis I.</i> Classification Based on Machine Learning of Fe i 7090A Spectra Derived from CO5BOLD Simulations	20
<i>Kozubek M., Küchelbacher L., Chum J., Lastovicka J., Podolska K., Sindelarova T., Trinkl F., Wüst S., Bittner M.</i> Preliminary Results: Lidar Measurements to Identify Streamers and Analyze Atmospheric Waves LISA (Aeolus+Innovation)	20
<i>Setsko P.V., Mingalev O.V., Artemyev A.V., Melnik M.N.</i> Estimation of the Current Sheet Parameters in Near-Jupiter's Magnetotail Using Simulation	21

Instrumentation for Space Weather Monitoring

<i>Bezrukovs V., Klokovs A.</i> Overview About VIRAC and Ongoing Activities	22
<i>Dachev T., Tomov B., Matviichuk Y., Dimitrov P., Semkova J., Koleva R., Jordanova M., Bankov N., Mitev M. Krastev K., Malchev S., Mitrofanov I., Litvak M., Kozyrev A., Golovin D., Reitz G., Header D.-P., Benghin V., Shurshakov V.</i> Overview of the Space Radiation Extreme Events Observed with Liulin Type Instruments	22

Solar Influences on the Lower Atmosphere and Climate

<i>Chapanov Ya.</i> Solar Influence on Ozone Variations over ENSO Regions	23
<i>Georgieva K., Kirov B.</i> Space Weather Effects on the Atmosphere	23
<i>Gospodinov D.</i> Colours of the eclipsed Moon - effects of stratospheric transparency and solar activity	24
<i>Göker Ü.D., Kobanoğlu B., Akçay Ç., İpek M., Eratılmış M.</i> The Statistical Analysis of Air Crash Investigations from 1918 to 2022 and Comparison with Geomagnetic Storms	24
<i>Kirov B., Georgieva K., Asenovski S.</i> Space weather and its effects on spacecraft charging	25
<i>Shirov G., Petrov N., Tsvetkov Ts.</i> Digitization of Meteorological Data Archives Collected in Bulgaria	25
<i>Tonev P.</i> Peculiar Atmospheric Electric Field Response at High Latitude to Three Major SEP Events in 2001 and Its Possible Interpretation	25
<i>Veretenenko S., Dmitriev P.</i> Long-Term Variability of North Atlantic Cyclone Tracks: Possible Influence of Solar Activity and Galactic Cosmic Rays	26
<i>Wysokinski A., Kobylinski Z.</i> Wavelet Analysis and Recurrence Plots of Oxygen Isotope and Paleotemperature Records from NGRIP Ice Core	26

Solar Effects in the Biosphere and Lithosphere

<i>Dobrica V., Demetrescu C., Isac A., Stefan C.</i> Assessment of the Space Weather Hazard over Romanian Territory	27
--	----

Sun and Solar Activity

Relationship between Solar Energetic Particles and Solar Flares during the 24th Solar Cycle

Calisir M.A. Kilcik A.

Department of Space Science and Technologies, Akdeniz University Faculty of Science, 07058, Antalya, Turkey

In this study, solar energetic particle (proton) and different class X-Ray solar flares were compared during the solar cycle 24 (2009-2019). We used 2-hour average proton intensities taken from different energy channels observed by SOHO/ERNE and solar flares detected by Konus-WIND. Monthly average data for each energy channel (1.8-3.3, 3.3-6.4, 6.4-13, 13-26, 26-51 MeV) were calculated during the investigated time period. The temporal variations of all data sets were compared and the correlation coefficients were calculated between different flare classes and proton intensities by using the cross correlation analysis methods. We found that proton intensities for all channels show the better agreement and the higher correlations with X class flares compared to other classes.

Different Prominence Eruptions and Associated Coronal Mass Ejections

Dechev M.¹, Koleva K.², Duchlev P.¹, Simic Z.³, Chandra R.⁴

¹Institute of Astronomy with NAO, BAS, Bulgaria

²Space Research and Technology Institute, BAS, Bulgaria

³Astronomical Observatory, Belgrade, Serbia

⁴Department of Physics, DSB Campus, Kumaun University, Nainital 263 002, India

Coronal mass ejections (CMEs) are closely related with prominence eruptions. Here we focus on the prominence eruptions (PEs) and their associated CMEs in six events. The presented events differ by the type, pre-eruptive conditions and eruption evolution. We calculate kinematic parameters of the eruption and discuss magnetic properties of the region of origin as a main factor for the specific PE and CME evolution.

Coronal Mass Ejection Effect on Interplanetary Medium: A Case Study

Demiroz M.I., Kilcik A.

Akdeniz University, Faculty of Science, Department of Space Sciences and Technologies

This study focuses on an Earth-directed high-speed CME event, structure of geomagnetic field and interaction between these phenomena. CME data taken from NASA SOHO/LASCO CME catalog and the selected high-speed (2147 km/s) earth-directed CME events occurred at 2014-02-25 were analyzed. The used geomagnetic indices, magnetic field components and magnitudes are taken from WDC Kyoto University website. Possible correlations between selected CME event and magnetic field components were obtained. All parameters (magnetic field components, geomagnetic activity indices, X-ray fluxes, charged particle properties, proton fluxes in different energy levels, flow pressure and bowshock nose location) have remarkable improvements during the investigated time period. We found that all these parameters and their variations which are recorded by the relevant spacecrafts and observatories, had impacts to the interplanetary space and the Earth in different ways.

Diagnostics of Solar Proton Events Based on the Parameters of Type II and IV Radio Bursts

Isaeva E.
STIL-BAS

A large sample of solar proton events was studied for the period from 1986 to 2018 years. This sample contains 349 proton events. For all 349 proton events, a regression model was found that gives a very good approximation for the integral energy spectrum of protons with energy E_p in the range $> 0.8 - 850$ MeV. Also, on the basis of a large sample of proton events, the conclusions of other authors were confirmed that the main acceleration of average relativistic solar protons occurs in the flare region and additional at the fronts of shock waves. However, further detailed studies of the relationship between the SCR proton flux and the parameters of type II radio bursts showed that there is a strong relationship between the SCR proton flux and the intensity of type II bursts in the range of 25–180 MHz. It was also found that there is a fairly strong relationship between the intensity of type II bursts and the maximum value of microwave bursts at a frequency of 8800 MHz. This fact, in turn, indicates that coronal shock waves are generated by solar flares. At the same time, it was shown that there is a strong relationship between the CME velocity and the integral flux of Type IV microwave bursts, which is in full agreement with the known model CSHKP (By first letters of authors' surnames Carmichael 1964; Sturrock 1966; Hirayama 1974; Kopp & Pneuman 1976).

Activity of Solar Twins

Katsova M.¹, Nizamov B.¹, Shlyapnikov A.²

¹Sternberg State Astronomical Institute, Lomonosov Moscow State University,

²Crimean Astrophysical Observatory RAS, Nauchny

We present an analysis of various tracers of magnetic activity for 23 solar twins which are characterized by significant scatter of lithium abundance in their atmospheres. A level of coronal and chromospheric activity has been studied from available X-ray and UV- archival data. It gives us a chance to compare coronae of solar twins of various ages with the solar case. We found a scatter in the X-ray to bolometric luminosity ratio L_x/L_{bol} by several orders of magnitude, which exists in these stars along with a significant spread in Li abundance. This may link the surface activity of stars with phenomena at the base of their convective zones. The TESS data allowed us to reveal rotation modulation of stellar brightness associated with starspots. For some twins of our samples, periods of axial rotation are detected around 6 days, i.e. these stars rotate almost 4 times faster than the contemporary Sun. This indicates their relative youth. Flare activity of solar twins is discovered in the TESS data; we showed existence of various kinds of flares, and present temporal profiles for some of them. We obtained the energy about of 8×10^{33} erg for the largest flare of our samples, lasting longer than 4 hours. In addition, we discuss also magnetic fields and properties of exoplanets, orbiting these stars.

A Comparison Between the Solar Activity in the 11-Year Sunspot Cycles During the Last Two Centennial Solar Activity Minima. A Comparison of the Geomagnetic Activity During the Same Periods

Kirov B., Georgieva K., Asenovski S.
Space Research and Technology Institute - BAS

When speaking about variations in solar activity, usually variations in the number of sunspots is meant. It is well established that there is an about 11-year cycle in the sunspot number. The beginning of a cycle is defined as the period of the sunspot minimum, which may be different in both duration and number of sunspots. After that, an increase in sunspot number follows reaching to a maximum, and again a decrease until the next minimum. Later, a quasi-centennial (“Gleissberg”) cycle was found. In about 100 years the maxima of the sunspot number in the 11-year cycles gradually increase to a centennial maximum, and then decrease to the next centennial minimum.

Now we know that sunspots are a manifestation of the solar toroidal magnetic field which is the source of the coronal mass ejections which cause the big sporadic (non-recurrent) geomagnetic storms. Therefore, during sunspot maximum there is also a maximum in geomagnetic activity. Another source of geomagnetic activity are the coronal holes – open unipolar magnetic field areas from which the high speed solar wind emanates. Disturbances caused by high speed solar wind are maximum during the sunspot declining phase, which leads to two geomagnetic activity maxima in the 11-year sunspot cycle.

In the present work, we compare the number of sunspots in the different phases of the last two 11-year cycles which belong to the present secular solar minimum, and compare them to the analogous period of the previous secular solar minimum about one century ago.

Forecast of the Solar and Geomagnetic Activity During 25 - 26 Cycles by Means of Elman ANN

Kobyliński Z., Wysokiński A.
High School of National Economics, Kutno, Poland
Independent researcher, Iganie, Poland

The purposes of the paper is the calculation of the solar number and geomagnetic index aa progression during the solar cycles 25 and 26 basing on the earlier cycles data from 11 cycle till the time of 2021 year by means of the Elman artificial neural networks. Thus the paper is an extension of the poster presented during 13th Workshop. For the period 1939 till present time we use also cosmic ray records as the additional indicator of activity. The wavelet technique and recurrence plots are used to show the coherence between studied data. This analysis shows a small increase of activity during the present and 26th cycles. Our study show also that Elman ANN can be successful technique for data forecast.

Solar Asymmetric Filament Eruption Observed by the Solar Dynamic Observatory and Related Activity

Koleva K.¹, Dechev M.², Duchlev P.², Chandra R.³

¹Space Research and Technology Institute - BAS

²Institute of Astronomy and National Astronomical Observatory - BAS

³Kumaun University, Nainital, India

An asymmetric eruptive prominence (EP) appeared on 2014 Nov 01 and it was followed by a two-ribbon solar flare. The ejection triggered a fast coronal mass ejection (CME) that was well visible in the LASCO C2 field of view. The morphology and kinematics of the EP and two-ribbon flare were examined by multi-channel observations from AIA/SDO and SoHO/LASCO. Initially, the EP slowly rose and then it sharply ejected up with a strong acceleration producing the CME bright core. The evolution of two-ribbon flare is morphologically characterized by separation of the two ribbons in the chromosphere. The ribbons' separation showed two-stage evolution: first one with relatively fast decelerating and very slow second one with low constant velocity. Such separating motion is believed to provide a signature of the reconnection process occurring progressively higher up in the corona.

Hidden Timescales in Solar and Stellar Flares

Kolotkov D.Y.

Centre for Fusion, Space and Astrophysics, University of Warwick, United Kingdom

The physics of flares remains an enigmatic question in plasma astrophysics, as the existing 'standard' model of a solar flare often fails to match the observed characteristic times, e.g. fast magnetic reconnection, without additional assumptions. A ubiquitous but not yet fully explored feature of solar flares, not predicted by the standard flare model, is quasi-periodic pulsations (QPP) which appear as quasi-periodic, usually short-lived modulation of the flare emission intensity in all spectral bands, associated with magnetohydrodynamic (MHD) oscillations and/or repetitive regimes of magnetic reconnection. We will overview the most recent achievements and outstanding questions in multi-band observational and theoretical studies of QPP. In particular, we will focus on their role in the standard flare model, including flare ignition, development, and possible link between different emission mechanisms. We will discuss natural physical scenarios by which an impulsive flare-caused excitation may lead to a quasi-periodic response from the host active region, such as MHD resonators and dispersion. We will also point out similarities between QPP events observed in solar flares and much more powerful stellar superflares, which opens up promising perspectives of solar-stellar analogies through the prism of QPP. We will show the effects of solar flare QPP events on the near-Earth conditions, resulting in a periodic QPP-driven modulation of the electron number density in the lower ionosphere. Continuing the analogy with the types of magnetospheric pulsations (Pc and Pi), we will indicate the need for establishing similar classification scheme for QPP in flares, based on their observational and theoretically predicted properties.

Structure of the Solar Corona During the Solar Cycle Rising Phase

Kostov M.

Space Research and Technology Institute, Bulgarian Academy of Sciences, Stara Zagora Department,
Stara Zagora, Bulgaria

Structure of the solar corona highly depends on the level of solar activity through a solar cycle. Its analysis gives an important knowledge about the solar magnetic fields, its evolution and origin. We have a series of ground based observations of total solar eclipses (TSE). Using high resolution eclipse pictures of the white light solar corona we create composite images for studying small- and large-scale structures and comparison with satellite photos. Here we consider 1999 and 2012 total solar eclipses, which are during the rising phase of solar cycle 23 and 24 accordingly.

Solar corona photographs in white light during the 1999 TSE are obtained by a large-aperture camera (200/1000mm and telescope 150/2250mm Meniskas - Cassegrain), and telescopes-refractors (63/840mm). Black and white professional photographic films Kodak T-MAX 200 Pro with unique structure are used.

During the 2012 TSE, solar corona is observed with 300 mm objective and 2000 mm Macsutov-Cassegrain telescope. Photos are made with different exposures in order to obtain high-resolution composite images. The eclipse observations are compared with near-simultaneous SOHO EUV and SOHO LASCO visible-light coronagraphic images.

Analysis of the Ludendorf flattening indices and phase of the solar cycle shows that white light corona is solar maximum type – the shape is spherical with many streamers located at all azimuths around the occulted disk.

Structures of the 1999 and 2012 corona are compared with the coronas observed during the 1936 and 1966 eclipses, which are also during the solar cycle rising phase of similar in yearly mean sunspot number cycles - 17 and 20 accordingly.

Solar Manifestations in the Martian Orbit Observed from the Liulin Instrument

Krastev K.¹, Semkova J.¹, Koleva R.¹, Benghin V.², Drobijshhev S.²

¹STILL-BAS,

²IMBP -RAS

This paper presents data from the Liulin-Exomars device for the last year. The connections between the most interesting solar events and the measurements of the instrument for the corresponding period were studied. Estimates of doses and fluxes of galactic cosmic rays at 1 au were made.

Pioneering Energetic Particle Observations Near the Sun by Solar Orbiter and Parker Solar Probe

Malandraki O.E.¹, Rodríguez-Pacheco J.², McComas D.J.³, Wimmer-Schweingruber R.F.⁴, Schwadron N.⁵, Ho G.C.⁶, Desai M.⁷, Mitchel D.G.⁶, Kollhoff A.⁴, Janitzek N.⁸, Pacheco D.⁴, Gomez-Herrero R.², Posner A.⁹, Kouloumvakos A.¹⁰, Dresing N.¹¹, Heber B.⁴, Cohen C.M.S.¹², Kuehl P.⁴, Leske R.¹², Wiedenbeck M.¹² and the Solar Orbiter/EPD and PSP/ISOIS teams.

¹National Observatory of Athens, IAASARS, Metaxa & Vas. Pavlou str., Pedeli, 15236, Athens, Greece

²Universidad de Alcalá, Alcalá de Henares, Spain

³Department of Astrophysical Sciences, Princeton University, Princeton, NJ 08544, USA

⁴Institut für Experimentelle und Angewandte Physik, Christian Albrechts-Universität zu Kiel, Germany

⁵University of New Hampshire, Durham, NH 03824, USA

⁶Johns Hopkins University, Applied Physics Laboratory, Laurel, MD 20723, USA

⁷University of Texas at San Antonio, San Antonio, TX 78249, USA

⁸European Space Astronomy Center, Villanueva de la Cañada, 28692 Madrid, Spain

⁹NASA/HQ, 300 Hidden Figures Way SW, Washington DC, 20546, USA

¹⁰IRAP, Université Toulouse III - Paul Sabatier, CNRS, CNES, Toulouse, France

¹¹Department of Physics and Astronomy, University of Turku, FI-20014 Turku, Finland

¹²California Institute of Technology, Pasadena, CA, USA

Solar Energetic Particles (SEPs) constitute an important contributor to the characterization of the space environment. They are emitted from the Sun in association with solar flares and Coronal Mass ejection (CME)-driven shock waves. SEP radiation storms may have durations from a period of hours to days or even weeks and have a large range of energy spectrum profiles. These events pose a threat to modern technology strongly relying on spacecraft, are a serious radiation hazard to humans in space, and are additionally of concern for avionics and commercial aviation in extreme circumstances. However, after decades of observations of SEPs from space-based observatories, relevant questions on particle injection, transport, and acceleration remain open. Understanding how the Sun accelerates particles to relativistic energies and how these propagate from their acceleration site to fill the heliosphere is one of the key questions that the Solar Orbiter (SoLO) ESA mission has set out to answer by means of the Energetic Particle Detector (EPD) measurements. Furthermore, the NASA Parker Solar Probe (PSP) mission also addresses key questions regarding SEP events, utilizing measurements by the Integrated Science Investigation of the Sun (ISOIS) instrument suite. In this talk, unique energetic particle observations obtained in the inner heliosphere by these two pioneering missions as well as the exciting new results derived will be presented, highlighting how SoLO and PSP observations are advancing our current knowledge and understanding of SEPs.

Variations of the Sunspot Groups Separation Distance and Tilt Angles During the Decay

Muraközy J.

Institute of Earth Physics and Space Sciences (ELKH-EPSS)

Continuing the study of the sunspot groups decays their motions will be discussed. The results obtained by using the most detailed sunspot catalog SOHO/MDI-Debrecen Sunspot Data. Altogether more than 140 different active regions are selected, and each of them fits the very strict selection method, which ensures that all of them are in their decaying phase. Temporal variation of the separation distances between polarity regions as well as the tilt angles are investigated by taken into account some properties (hemispheric location, area dependence, etc.). As a result of this study one can conclude that the sunspot groups with different areas behave differently during their decay. This is the case of the northern and southern groups as well. The largest groups show the largest separation and tilt angle and their values change the steepest during the decay, while the smallest and middle-size groups vary slower. A connection between tilts and decay rates of groups can also be pointed out, the more tilted groups show higher the decay rates, and the average tilt angle increases with the polarity separation distance.

This research leading these results is funded by National Research, Development and Innovation Office – NKFIH, under grant agreement 141895.

Clarifying Physical Properties of Magnetic Fields in Sunspots

Obridko V.N.¹, Katsova M.M.², Sokoloff D.D.³, Shelting B.D., Livshits I.M.

¹IZMIRAN, 4 Kaluzhskoe Shosse, Troitsk, Moscow, 142190

²Sternberg State Astronomical Institute, Lomonosov Moscow State University, Universitetskij prosp.13, Moscow, 119991, Russia

³Moscow State University, Moscow, 119991, Russia

From the very beginning and long afterwards, the number and area of sunspots were determined visually from solar images based on their photometric properties. Nowadays, we are using photo and numerical records. There is no doubt, however, that the main factor determining the very existence of a sunspot is the magnetic field. Nevertheless, a definition of the sunspot boundary in terms of the magnetic field is still absent in scientific literature. Here, we suggest such a definition based on SDO/HMI observations. We demonstrate that the radial magnetic field component at the outer boundary of the penumbra is about 550 Mx/cm² independent of the sunspot area and the maximum magnetic field in the umbra. The mean magnetic field intensity in sunspots grows slightly as the sunspot area increases up to 500-1000 m.v.h. and may reach about 900–1300 Mx/cm². The total magnetic flux weakly depends on the maximum field strength in a sunspot and is determined by the spottedness, i.e., the sunspot number and the total sunspot area; however, the relation between the total flux and the sunspot area is substantially nonlinear.

Temporal and Periodic Variations of the Solar Flare Index during Last Four Solar Cycles and their Association with Selected Interplanetary Parameters

Ozguç A.¹, Kilcik A.², Yurchyshyn V.³

¹Kandilli Observatory and Earthquake Research Institute, Bogazici University, 34684 Istanbul, Turkey

²Department of Space Science and Technologies, Akdeniz University Faculty of Science, 07058 Antalya, Turkey

³Big Bear Solar Observatory, New Jersey Institute of Technology, Big Bear City, CA 92314, USA

We studied temporal and periodic variations of monthly solar flare index (FI) and selected geomagnetic activity indices (Ap, Dst, Scalar B and aa) measured during solar cycles 21- 24 (from January 1, 1975 to December 31, 2020) and report the following findings. 1) All data sets except FI peak values were gradually decreasing since 1992, while the FI peak values began their gradual decrease in 1982. 2) All data sets show double or multiple peaks during the maximum phase of solar cycles and the time of maxima generally coincide. 3) FI shows meaningful correlations with the investigated interplanetary indices. 4) The 11 year sunspot cycle periodicity and as well as periodicities lower than 3.9 months were observed in all data sets without exception. 5) FI time series exhibit a unique period of 4.8 – 5.2 month that is not present in all other indices, while geomagnetic aa, Ap and Dst indices show a unique 6-6.1-month periodicity that does not appear in the scalar B and FI indices. 6) XWT spectrums between FI and other indices generally show phase mixing at the short (2-8 months) period range, while all indices used in this study were found to be in phase and highly correlated with the 11 years solar activity periodicity.

Singularities of the Magnetic Field Configuration During Flares M1.4 on May 27, 2003 at 02:43 and M 1.9 on May 26, 2003 at 05:34 According to the Results of MHD Simulation Above the Active Region AR 10365

Podgorny A.I.¹, Podgorny I.M.², Borisenko A.V.¹

¹Lebedev Physical Institute RAS

²Institute of Astronomy RAS

The MHD simulation of a flare situation in the solar corona above a real active region (AR) is continued in order to study the physical mechanism of a solar flare and, in the future, improve the prediction of solar flares based on an understanding of their physical mechanism. Studies have once again confirmed that the only mechanism that can explain the slow accumulation of magnetic energy in the solar corona and then its rapid release during a flare is the mechanism of the release of energy accumulated in the magnetic field of the current sheet. The results of recent studies lead to the conclusion that the study of the flare mechanism is impossible without MHD simulation above a real active region, in which the calculation begins several days before the appearance of flares, when the magnetic energy for the flare has not yet accumulated in the corona. For MHD simulation in the real scale of time, it is necessary to carry out parallel calculations, which were performed by computational threads on graphics cards (GPUs) using CUDA technology. MHD simulation showed the appearance of current sheets on singular lines, in the vicinity of which the magnetic field has an X-type configuration. In addition, in the vicinity of a significant number of singular lines, a divergent magnetic field (magnetic trap field) is superimposed on the X-type magnetic field configuration. In such an overlay of configurations, even if the divergent field predominates, a sufficiently powerful current sheet can form due to the presence of an X-type field. The flare mechanism based on the accumulation of energy in the magnetic field of the current sheet is confirmed by the coincidence of the positions of singular magnetic lines, in the vicinity of which current sheets are formed, with the observed positions of the flares M1.4 on May 27, 2003 at 2:43 and M 1.9 on May 26, 2003 at 05:34 above AR 10365.

Observation of Solar Energetic Particle Events Onboard ExoMars TGO in July 2021-March 2022

Semkova J.¹, Koleva R.¹, Benghin V.³, Krastev K.¹, Matviichuk Y.¹, Tomov B.¹, Bankov N.¹, Maltchev S.¹, Dachev T.¹, Mitrofanov I.², Malakhov A.², Kozyrev A.², Golovin D.², Mokrousov M.², Sanin A.², Litvak M.², Nikiforov S.², Lisov D.², Anikin A.², Shurshakov V.³, Drobyshv S.³

¹Space Research and Technology Institute, Bulgarian Academy of Sciences, Sofia, Bulgaria

²Space Research Institute, Russian Academy of Sciences, Moscow, Russia

³State Scientific Center of Russian Federation, Institute of Biomedical Problems, Russian Academy of Sciences, Moscow, Russia

The dosimetric telescope Liulin-MO for measuring the radiation environment onboard the ExoMars TGO is a module of the Fine Resolution Epithermal Neutron Detector (FREND).

Here we present results from measurements of the charged particle fluxes and dose rates at ExoMars TGO science orbit (circular orbit with 400 km altitude, 74° inclination, 2 hours orbit period), provided by Liulin-MO since May 2018. The period of measurements covers the declining and minimum of the solar activity in 24th solar cycle and the inclination phase of the 25th cycle.

Particular attention is drawn to the observation of the solar energetic particle (SEP) events in July, September and October 2021, February and March 2022 as well as their effects on the radiation environment on TGO during the corresponding periods. The SEP event on 15-19 February 2022 is the most powerful event observed in our data. Compared are the time profiles of the particle fluxes and count rates measured by Liulin-MO and the neutron detectors of FREND during these events. The data for SEP events on TGO in July 2021-March 2022 contribute to the details for the solar activity at a time when Mars is on the opposite side of the Sun from Earth.

Acknowledgements: The work in Bulgaria is supported by grant KP-06 Russia 24 for bilateral projects of the National Science Fund of Bulgaria and Russian Foundation for Basic Research.

Stellar Dynamo and Structure of Current Sheets

Sokoloff D., Malova Y., Maiewsky E., Yushkov E., Popov V.

Moscow State University and Space Research Institute

Dynamo action in a star produces magnetic field around the star which in turn determines current sheet structure in the space surrounding the star. The point however is that stellar dynamos can in principle produce various magnetic configuration. We discuss how a dynamo supported magnetic configuration is related to the current sheets configuration.

Database of Solar Cycle 24 Coronal Mass Ejections and Flares Related to Active Regions

Tsvetkov Ts.¹, Nakeva Y.², Petrov N.¹

¹Institute of Astronomy and National Astronomical Observatory, Bulgarian Academy of Sciences

²Department of Physics, Aix-Marseille University

We present an online database of coronal mass ejections (CMEs) and solar flares (SFs) associated with active regions (ARs). The time range of the collected data lays in the period of solar cycle 24 (December 2008 – December 2019). Used sources of information include NOAA Space Weather Prediction Center AR list, GOES soft X-ray flare listings and SOHO LASCO CME Catalog. Overall, 1533 ARs that produced at least one SF and/or CME are involved in our catalog together with their coordinates and Hale class for each day they were observed on the solar disk as well as data for the onset, central position angle, angular size and speed (of associated CMEs) and class, start, peak and end times (of AR-related SFs).

Possible Causes and Consequences of the Weakening of the Solar Wind in the Current Epoch of the Grand Solar Minimum

Yermolaev Y.I., Lodkina I.G., Khokhlachev A.A., Yermolaev M.Yu., Riazantseva M.O., Rakhmanova L.S., Borodkova N.L., Sapunova O.V., Moskaleva I.A.V.

¹ Space Research Institute (IKI), RAS

Using data of the OMNI catalog (<https://pdf.gsfc.nasa.gov/pub/data/omni>) and the catalog of large-scale solar wind phenomena (<http://www.iki.rssi.ru/pub/omni>), we showed that with the beginning of the era of the grand minimum of solar activity, the parameters of the solar wind (except for the velocity) noticeably (by 20–40%) decreased both in various large-scale solar wind phenomena and in various phases of the solar cycle, and they remained low in cycles 23 and 24 [Yermolaev et al., JGR, 2021 <https://doi.org/10.1029/2021JA029618>; Yermolaev et al., Proc. 2021 DOI: 10.31401/WS.2021.proc]. The number of CMEs and their manifestations in the interplanetary medium (sheaths and magnetic clouds) also dropped noticeably, while the number of fast streams from coronal holes and their distributions (CIRs) remained the same. In this report we discuss possible conclusions on the physics of the Sun, solar wind, magnetosphere and space weather, which follow from the data obtained.

The work was supported by the Russian Science Foundation, grant 22-12-00227.

Temporal and Latitudinal Distribution of Anti-Hale Active Regions in the Synthetic Solar Cycle

Zhukova A.¹, Khlystova A.², Abramenko V.¹, Sokoloff D.^{3,4,5}

¹CrAO RAS

²ISTP SB RAS

³MSU

⁴MCFAM-MSU

⁵IZMIRAN

We used long observational series for bipolar active regions (ARs) to study aspects of the mutual transformation of the poloidal and toroidal components of the global solar magnetic field. The direction of the toroidal field determines the polarity of leading sunspots in ARs. The vast majority of bipolar ARs obey the Hale's polarity law, whereas some ARs have the opposite sense of polarity (anti-Hale ARs). However, the study of these ARs is hampered by their poor statistics. The data for five 11-yr cycles (16–18 and 23, 24) were combined to compile a synthetic cycle of unique time length and latitudinal width. The synthetic cycle comprises data for 14838 ARs and 367 of them are the anti-Hale ARs. A specific routine to compile the synthetic cycle was demonstrated. We found that, in general, anti-Hale ARs follow the solar cycle and are spread throughout the time-latitude diagram evenly, which implies their fundamental connection with the global dynamo mechanism and the toroidal flux system. The increase in their number and percentage occurs in the second part of the cycle, which is in favour of their contribution to the polar field reversal. The excess in the anti-Hale ARs percentage at the edges of the butterfly diagram and near an oncoming solar minimum (where the toroidal field weakens) might be associated with the strengthening of the influence of turbulent convection and magnetic field fluctuations on the arising flux tubes. The evidence of the misalignment between the magnetic and heliographic equators is also found.

Solar Wind-Magnetosphere-Ionosphere Interactions

Toward the Space Climate Characterization of the Heliosphere – Magnetosphere Environment for the Last 400 Years

Demetrescu C., Dobrica V., Stefan C.
Institute of Geodynamics, Romanian Academy

The space climate is the long-term change in the Sun, and its effects in the heliosphere and upon the Earth, including the atmosphere and climate. In this paper we infer the evolution of space climate in the past based on space and geomagnetic data, reviewing some of our previous results on the matter. As the instrumental space research began only in 1964, we rely also on solar activity reconstructions. As regards the geomagnetic data, it is well known that (1) the study of geomagnetic phenomena known as geomagnetic activity has long contributed to progress in solar-terrestrial science and (2) the long geomagnetic time series recorded at geomagnetic observatories have provided means to characterize the Sun-Earth interaction at times prior to space era, via geomagnetic indices. An important output of the paper regards the role of magnetospheric and ionospheric currents in inducing components of long-term secular variation of the geomagnetic field.

Relationship Between the Intense Mid-Latitude Geomagnetic Effect at the Panagurishte Station and Solar Wind Conditions

Despirak I.V.¹, Werner R.², Lubchich A.A.¹, Kleimenova N.G.³, Guineva V.²

¹Polar Geophysical Institute, Apatity, Russia

²Space Research and Technology Institute, Bulgarian Academy of Sciences, Stara Zagora Department, Bulgaria

³Schmidt Institute of Physics of the Earth, RAS, Moscow, Russia

The purpose of this work is to find out solar wind conditions under what high values of the horizontal power of the magnetic field (MPB) are observed at the Panagurishte station in Bulgaria. In 2007-2018, about of 40 events of high MPB values (> 2000 nT²) were identified. Each event was compared with the presence of a substorm in the auroral zone, its development, and intensity. The study of the substorm occurrence was based on the data from the magnetometer networks SuperMAG, INTERMAGNET and IMAGE. The solar wind conditions before the substorms were determined using the CDAWeb OMNI database (<http://cdaweb.gsfc.nasa.gov/>), the solar wind structures were determined according to the catalog of large-scale solar wind phenomena (<ftp://ftp.iki.rssi.ru/omni/>). It turned out that strong surges in the MPB were observed during intense substorms (AL-index $\sim 700-1700$ nT; IL-index $\sim 400-1100$ nT). Moreover, about the half of these substorms were the so-called “high-latitude” substorms, which propagated in its progress to the geomagnetic latitudes higher than $\sim 70^\circ$ CGCLAT. Many events of strong peaks in the MPB were registered during the main phase of the magnetic storm, caused by Corotating Interaction Region (CIR) in the solar wind, and before their appearance the jump in the solar wind dynamic pressure was observed. So, it was shown that strong MPB peaks were connected mainly with intense substorm events observed during solar wind high-speed streams from coronal holes.

This study was supported by the RFBR (project number 20-55-18003) and National Science Fund of Bulgaria (NSFB) (project number КП-06-Русия/15).

Supersubstorm on 20 December 2015: Spatial Geomagnetic Effects

Despirak I.V.¹, Lubchich A.A.¹, Kleimenova N.G.², Setsko P.V.¹, Werner R.³

¹Polar Geophysical Institute, Apatity, Russia

²Schmidt Institute of Physics of the Earth, RAS, Moscow, Russia

³Space Research and Technology Institute, BAS, Stara Zagora Department, Bulgaria

We analyzed the supersubstorm (SML- index ~2100 nT) observed on December 20, 2015 (onset at ~ 16:10 UT) during the intense magnetic storm caused by the magnetic cloud (MC), which included a stable southward Bz IMF direction. It is shown that the ionospheric currents, corresponding to this supersubstorm, developed on a global scale, from the evening to the late morning sectors. During its development, the very intense westward electrojet was observed with the maximum in the morning sector (~06 MLT). In the evening sector (~18 MLT), the strong eastward electrojet was observed. During the expansion phase of the substorm in the evening sector, variations in the magnetic field were observed, corresponding to the appearance of an additional current wedge in the opposite direction. Moreover, we obtained the auroral oval location for this event using data from NOAA(POES) satellites. It was shown that the spatial development of the westward electrojet corresponded to the auroral oval location. The development of the substorm was accompanied by the appearance of a large positive variation in the X component of the magnetic field at geomagnetic latitudes from ~60° to ~50°, which could lead to the observed pulse of the MPB index (Midlatitude Positive Bay index). Thus, this supersubstorm demonstrated its global behavior accompanied an addition substorm current wedge development.

This study was supported by the RFBR (project number 20-55-18003) and National Science Fund of Bulgaria (NSFB) (project number КП-06-Русия/15).

Ground-Based Pc1 Geomagnetic Pulsation Polarization as a Proxy of the Plasmopause Location

Feygin F. Z., Khabazin Yu. G., Kleimenova N. G., Malysheva L. M.

Institute of Physics of the Earth, RAS, Russia

The typical magnetospheric ion-cyclotron waves are observed on the Earth's surface as Pc1 geomagnetic pulsations in the 0.2–5 Hz range. The Pc1 pulsations are generated by cyclotron instability of the protons of the Earth radiation belt in the equatorial plane of the magnetosphere in the form of Alfvén left-hand polarized waves. Here we present the scenario of the Pc1 pulsation propagation from the region of their generation in the magnetosphere (most likely in vicinity of the plasmopause) to a ground-based receiver, including the ionospheric waveguide (in the F2 layer). The waves propagate in this waveguide horizontally over long distances in latitude and longitude with very little attenuation, but herewith the left-hand polarized waves very rapidly attenuate with a distance, and the left-hand polarized waves transform into the right-hand polarized, fast magnetosonic waves. Thus, on the ground, near the plasmopause projection, the polarization of the Pc1 geomagnetic pulsations should be left-handed. We carried out the analysis of the latitudinal distribution of the about 200 events of Pc1 wave polarization at the Scandinavian chain of induction magnetometers and confirmed that wave polarization can use as a natural proxy of the location of the plasmopause projection.

Effect of Solar Wind Density in the Time Structure of Geomagnetic Storms

Gopalswamy N.¹, Yashiro S.^{1,2}, Xie H.^{1,2}, Akiyama S.^{1,2}, Mäkelä P.^{1,2}

¹NASA/GSFC

²Catholic U

Successive intervals of southward interplanetary magnetic fields arriving at the magnetosphere are thought to be the main cause of multiple-dip storms. Occurrence of southward field in both the sheath and cloud portion of interplanetary CMEs (ICMEs) separated by a less geoeffective interval is the most common cause of multiple-dip storms. Such a scenario can also develop due to successive ICMEs. Here we report on a different kind of time structure in the storm main phase attributed to the density structure in shock sheath, CME flux rope, and in CIR. One of the common features is the sudden steepening of the Dst time profile when the solar wind density increases while the interplanetary magnetic field has a southward component. The slope change can also lead to storm weakening when the density drops significantly. The Dst index is better correlated with the integral of the ring current injection rate that incorporates solar wind density. The main-phase time structures are important because they represent variations in Earth's magnetic field and hence lead to variability in geomagnetically induced currents.

Polar Geomagnetic Disturbances and Auroral Substorms During the Magnetic Storm on 20 April 2020

Gromova L.I.¹, Kleimenova N.G.², Despirak I.V.³, Lubchich A.A.³, Gromov S.V.¹, Malysheva L.M.²

¹IZMIRAN, Moscow, Troitsk, Russia

²Schmidt Institute of Physics of the Earth RAS, Moscow, Russia

³Polar Geophysical Institute, Apatity, Russia

Global features of the spatial-temporal distribution of high-latitude geomagnetic disturbances in the first magnetic storm (20 April 2020) of the new, 25-th cycle of the solar activity were studied. Our analysis was based on the data from the ground-based stations of the global Intermagnet and SuperMAG nets as well as the Scandinavian meridional IMAGE chain. This storm initial phase demonstrates some non-typical behavior. The long lasting period (of about 2 hours) when IMF Bz remained negative, is untypical for the initial phase of a magnetic storm. It led to the small substorm developing in the night sector of the high-latitudes accompanied by the mid-latitude positive magnetic bays. Two local vortex structures were observed in this time concentrating at the high latitudes (>65° MLAT): a negative vortex in the near-midnight sector and positive one in the after-noon sector. They could be interpreted as the indicators of the local enhancements of the high-latitude field aligned currents (FACs) directed outward and inward respectively. Near the end of the storm initial phase, the daytime polar magnetic bay, controlled by the IMF By sign was observed under the predominantly positive IMF Bz. This bay did not accompanied by a positive bay in the mid-latitudes indicating that the source of the considered dayside magnetic bay did not related to a substorm current wedge developing. Probably, the bay was a result of intensification of FACs associated with the positive IMF Bz. Despite this magnetic storm was not strong, three very intensive (up to 1000 nT) magnetospheric substorms were observed at the during the storm main phase. These substorms were accompanied by a significant eastward electrojets recorded in the after-noon sector demonstrating the feature typical for a supersubstorm. That allows us to suppose the appearance of an additional substorm current wedge similar to supersubstorm one.

This study was supported by the RFBR (project number 20-55-18003) and National Science Fund of Bulgaria (NSFB) (project number KII-06Русия/15).

Maps of the Spatial Distribution of the Variations in the X and Y Components of the Magnetic Field at European Midlatitudes During Substorms: A Case Study

Guineva V.¹, Werner R.¹, Bojilova R.², Atanassov A.¹, Raykova L.¹, Valev D.¹

¹Space Research and Technology Institute (SRTI), BAS, Stara Zagora Department, Bulgaria

²National Institute of Geophysics, Geodesy and Geography (NIGGG), BAS, Sofia, Bulgaria

The goal of this work is to present the utility of maps of the magnetic field components variations to define the characteristics of the magnetospheric substorms appearance at midlatitudes. To study the spatial distribution of the magnetic field components variations during substorms, an isolated substorm, the substorm on 22 March 2013 at ~23:12 UT with central meridian over Europe has been chosen. Magnetic field data from INTERMAGNET, SuperMAG and IMAGE databases have been used. The X and Y variations due to the substorm were computed for 50 stations based on the developed programs. Maps of the spatial distribution of the magnetic variations have been created and some characteristics as the line of sign conversion latitude, the central meridian, the longitudinal and latitudinal extent of the positive bays and the latitudinal and longitudinal dependence of the variations at the time of the midlatitude positive bay maximum at Panagjurishte (PAG) have been estimated. The central meridian is near PAG (~37°MLAT). The sign conversion latitude is about 58°MLAT, the latitudinal extent – about 44°, and the longitudinal extent – about 78°. These results are typical for expanded substorms. The midlatitude local time profiles for this event have been constructed. The European midlatitude positive bay (MPB) index has been computed.

This study was supported by the National Science Fund of Bulgaria (NSFB) (project number КП-06-Русия/15) and by the RFBR (project number 20-55-18003).

Comparison of Ionospheric and Geomagnetic Anomalies over Bulgaria during St. Patrick's Geomagnetic Storm

Jivov I., Bojilova R.

National Institute of Geophysics, Geodesy and Geography, Bulgarian Academy of Sciences

This study presents ionospheric anomalies and variations in X and Y components of Earth's magnetic field over Bulgaria during geomagnetic storms of solar origin in 17–19 March 2015. The response of the ionosphere is considered by data from the ionosphere station Sofia at National Institute of Geophysics, Geodesy and Geography- Bulgarian Academy of Sciences NIGGG- BAS. Other used ionospheric quantity is Total Electron Content (TEC) provided by the Center for Orbit Determination of Europe (CODE). The variation in X and Y components are based on data of Panagyurishte station, which is part of the global network of observatories, monitoring the Earth's magnetic field - INTERMAGNET. The results of the investigation can help both to study the impact of geomagnetic storms on humanity and to create empirical models for predicting critical frequencies of the ionosphere.

Comparison of the Critical Frequencies of the Ionospheric F1 and F2 Layers with the X-Ray Solar Flare Numbers Observed during the Solar Cycle 24

Kilcik A., Tirnakci M.

Akdeniz University Faculty of Science, Department of Space Science and Technologies, 07058, Antalya, Turkey

In this study, the total monthly X-ray solar flare (SF) numbers observed during the 24th solar cycle (2008-2020) were compared with the monthly median critical frequencies of ionospheric F1 and F2 layers by using the temporal variation, cross-correlation and hysteresis analysis. The monthly median ionospheric critical frequency data are taken from the UK Solar System Data Center-Sodankyla (67°N,26°E), the daily X-ray Solar flare data are taken from the Laboratory for Experimental Astrophysics (LEA). We found following results; the temporal variation analysis show that, the critical frequency of F1 layer and the monthly total SF, C and X class solar flares number seem to be quite compatible. The critical frequency of the F2 layer show good agreement with total, C and M class solar flare numbers. Both F1 and F2 layers critical frequencies show very high positive correlation with total solar flare number with zero-time delay. ($r=0.89$, $r=0.96$, respectively). It has been observed that the separation between the hysteresis analysis and the path shows different cyclic behaviors that, the critical frequency of the F1 layer has a wider cycle than the critical frequency of the F2 layer.

Solar Magnetic Field and Earth Rotation

Kirov B., Georgieva K.
SRTI-BAS

It has long been known that the Earth rotation rate, or the length of the day (LOD), varies on different time-scales - from centuries to days. The secular deceleration of the Earth's rotation is primarily attributed to tidal friction in the oceans. On decadal time scales, the variations in LOD are correlated with variation in the geomagnetic field driven by processes in the core and the mantle. On time scales of up to several years the LOD variations are related to variations in the large-scale atmospheric circulation.

In the present work we look for a possible influence of solar activity on the LOD variations. We first compare the variations of the photospheric magnetic field and the interplanetary magnetic field (IMF) at the Earth's orbit. The IMF magnitude has a clear 11-year cycle while the photospheric magnetic fields in the two hemispheres exhibit the 22-year Hale magnetic cycle which is also characteristic for the IMF components. This 22-year cycle is also evident in the LOD variations. LOD is maximum in sunspot minimum between an even and odd sunspot cycle, and is minimum in sunspot minimum between an odd end even sunspot cycle. Because of this 22-year cycle in LOD and the 11-year cycle in the IMF magnitude, the correlation between the two varies – it is positive in negative polarity solar cycles (from odd sunspot cycle maximum to even sunspot cycle maximum) and negative in positive polarity solar cycles (from even sunspot cycle maximum to odd sunspot cycle maximum).

Morning Polar Substorms and Their Possible Mid-Latitude Effects

*Kleimenova N.G.¹, Despirak I.V.², Malysheva L.M.¹, Gromova L.I.³, Lubchich A.A.², Guineva V.⁴,
Werner R.⁴*

¹IPE-RAS

²PGI

³IZMIRAN-RAS

⁴SRTI-BAS

At high magnetic latitudes (above $\sim 70^\circ$ MLAT), there are the specific types of magnetospheric substorms observed in the local morning (at 08-09 MLT) under the absence of magnetic activity at lower latitudes. The morning polar negative magnetic bays are observed under both positive and negative IMF Bz, but the spatial distribution and nature of these bays should be different. The negative polar bays, recorded under the northward IMF (positive IMF Bz), could be associated with the azimuthal expansion of, so called, daytime polar substorms, controlled by the By IMF and associated with NBZ-type of the field aligned currents (FAC). As a rule, these morning bays do not accompanied by mid-latitude effects. Some morning polar bays observed under negative IMF Bz can be a result of the azimuthal expansion of a classical night substorm to the morning site. In this case, the morning polar substorm is accompanied by mid-latitude positive bay. However, another type of a morning polar substorm, observed after long lasting non-variable negative Bz IMF and under the absence of substorms in the near-midnight region, could be attributed to a developing of a, so called, convection substorm. In this case, there were no positive mid-latitude magnetic bays. Such situation could be interpreted as the absence of a substorm current wedge development.

This study was supported by the RFBR (project number 20-55-18003) and National Science Fund of Bulgaria (NSFB) (project number КП-06-Русия/15).

Ionospheric Variability Observed During 4 November 2021 Geomagnetic Storm

Koucká Knížová P.¹, Podolská K.¹, Mošna Z.¹, Kouba D.¹, Potužníková K.²

¹Institute of Atmospheric Physics, Dept. of Ionosphere and Aeronomy, Czech Academy Sciences

²Institute of Atmospheric Physics, Dept. of Meteorology, Czech Academy Sciences

Geomagnetic storms belong to the most pronounced manifestations of solar activity within ionospheric plasma. The response depends on the ionospheric system memory and type of the solar disturbance. In October and November we have observed several types of solar activity phenomena during relatively short period. It involves solar flare, radio emission and coronal mass ejection. On 28 October at 15:35 UTC a long duration X1.0 solar flare exploded from an Earth-facing position. It was the second X-class solar flare of Solar Cycle 25. This flare was associated with both Type IV and II radio emissions. It was followed by the coronal mass ejection. The leading edge of the X1.0 coronal mass ejection (CME) passed on 31 October at 09:13 UTC. Entire X1.0 coronal mass ejection has arrived at Earth at 12:31 UTC. Subsequently an M1.7 (R1 minor) solar flare with CME erupted on 1 November 2021 at 01:45 UTC and peaked at 03:01 UTC, and arrived on 3 November around 19:30 UTC. This combined with the high solar wind speed caused strong G3 (Kp7) geomagnetic storm conditions on 4 November. The plasma flow in the horizontal direction increased on 3 November. Ionization within F2 layer significantly decreased during on 4 November and returned to the normal values on 5 November. Entire F2 layer profile moved upward. The return to the regular height was accompanied by large wave-like oscillation of the entire profile. In detail we will present the behavior of all three components of the plasma drift.

Appearance of GICs in Case of Two SuperSubStorms on September 7 and 8, 2017

Setsko P.V.¹, Despirak I.V.¹, Sakharov Ya.A.¹, Bilin V.A.¹, Selivanov V.N.²

¹Polar Geophysical Institute, Apatity, Russia

²Northern Energetics Research Centre KSC RAS, Apatity, Russia

Amplitude and phase fluctuations of a field of an incident electromagnetic wave arise when the radiation passes through a plasma layer with electron density inhomogeneities. This phenomenon is found in interstellar medium, interplanetary plasma and in the Earth's ionosphere when radio astronomy observations are carried out. Such amplitude and phase scintillation significantly impact on radio astronomy studies at low frequencies and should be taken into account during the observations and data reduction. Ionospheric scintillation affects an accuracy of radio astronomy observations most severely. On the other hand, observational data distorted by the scintillation provide information on parameters of the scattering medium itself. We observed powerful radio sources with the URAN decameter interferometer network to study a temporal and spatial variation of the ionospheric scintillation in order to determine their relationship with terrestrial phenomena and space weather. We found, that an increase of the ionospheric scintillation measured by the UTR-2 radio telescope coincide with disturbances in the solar wind detected by space laboratories in Earth's orbit and with the URAN interferometers.

Assessing the Possible Sources of the Geomagnetic Storms By Means of Empirical Orthogonal Function Analysis

Stefan C., V. Dobrica V., Demetrescu C.

Institute of Geodynamics, Romanian Academy, Bucharest, Romania

This study is an attempt to identify the sources accountable for the perturbations observed in geomagnetic data for three major storms of solar cycle 24 (17 March 2015, Dst=-222 nT; 8 September 2017, Dst=-124 nT; 26 August, Dst=-174 nT) and for the 4th November 2021 (Dst=-105 nT), the only major storm until now of solar cycle 25. Data from the SuperMAG database for the northern hemisphere were analyzed using the empirical orthogonal function method (EOF). Further, the wavelet coherence analysis was used to assess the link between the time series of the EOF modes and various geomagnetic indices (Dst, AE, PC) that describe current systems in the magnetosphere and ionosphere, sources of perturbations. The results show that the main cause (45-68%) for the perturbations observed in data is given by the increase of the ring current during the storms.

Mid-Latitude Response to Auroral Substorms in Magnetic Field Variations at the Bulgarian Station Panagjurishte from 2007 Up to 2020

Werner R.¹, Guineva V.¹, Atanassov A.¹, Bojilova R.², Raykova L.¹, Valev D.¹, Despirak I.V.³,
Lubchich A.A.³, Kleimenova N.G.⁴, Setsko P.V.³

¹STIL-BAS

²NIGGG-BAS

³PGI-RAS

⁴UIPE-RAS

"The Bulgarian station Panagjurishte (PAG, corrected geomagnetic coordinates 42.7 N, 98.4 E) is located a little westward from the average location of the meridional chain of IMAGE stations from Polesie (PPN, 47.1 MLAT) to Ny Ålesund (NAL, 76.6 MLAT). The INTERMAGNET magnetometer network has collected the 1-min digital data from the Panagjurishte station since 2007. The data of the perturbations in X and Y magnetic field components as well as the horizontal power at Panagjurishte have been computed up to 2020 basing on the algorithms developed by Chu and McPherron. The details of the applied technique are briefly described. We used the IMAGE substorm index $IL_{<-200}$ nT for the IMAGE station chain from Polesie to Sørøya (SOR, 67.4 MLAT) as a proxy of the substorm occurrence at auroral latitudes and the chain PPN-NAL, which includes polar substorms. It was studied the nearly simultaneous appearance of positive magnetic bays at PAG with a perturbation of the X-component higher than 5 nT and substorms defined by IL. It was found out, that more than 70% of such substorms have been accompanied by positive magnetic bays at PAG. However, the PAG response to the polar substorms observed at IMAGE chain at stations higher than the SOR station was much lower. As to be expected, a relatively lower response of about 60% of the substorm events was found for the PPN-NAL chain, because this substorms number includes polar substorms as well. Substorms not accompanied by a positive bay are characterised by an exponential density distribution. Substorms accompanied by positive bay follow alike a Weibull distribution.

This study was supported by the National Science Fund of Bulgaria (NSFB) (project number КП-06-Русия/15) and by the RFBR (project number 20-55-18003).

Data Processing and Modelling

Analyse of Ionospheric and Geomagnetic Pre - earthquake Anomalies

Adibekyan M.

Ministry of Emergency Situations of the Republic of Armenia Territorial Survey for Seismic
Protection State Non-Commercial Organization

Aiming at earthquake precursors apportionment the earthquake preparation displays of ERZRUM (Turkey, 28.03.2004, M=5.4) and NOEMBERYAN (Armenia, 20.06.2008, M = 3.4), earthquakes in time-series have been studied using the geomagnetic and ionosphere tools. Aiming at earthquake forecasting the anomaly in the ionosphere plasma is investigated by a radio-astronomical method. There were received some results, allowing to make out the difference of seismogenic anomalies of ionosphere between the longer anomalies connected to magnetic activity of ionosphere by the method of vertical reconnaissance of ionosphere. For the analysis of geomagnetic time series used Pushkov's method. Results of the analysis observation have confirmed communication between earthquakes magnitude $M > 3.0$ and between and geomagnetic parameters. Have been investigated earthquakes of Noyemberyan (Armenia, 20.06.2008, M = 3.4). Have been used geomagnetic stations of observation Artik, Aruch and Djermuk There have been used the time – series Saravand ionospheric station.

Open Access Database for Different Types of Solar Wind

Asenovski S., Georgieva K., Kirov B.

Space Research and Technology Institute, Bulgarian Academy of Sciences

The presented open access database summarizes different types of solar wind and their duration in the near-Earth space, including high-speed solar wind streams and slow solar wind. The categorization of the different flows is based on criteria related to experimental data of the main solar wind parameters. The database uses physical conditions to clearly define the beginning and end of each event. The aim of this database is to cover the last four 11-year solar cycles (cycles 20 to 24 and partially 25) for which there are in situ satellite observations.

The Methodology for Calculating the Values of Monthly Median Critical Frequencies of E-Region

Bojilova R., Mukhtarov P.

National Institute of Geophysics, Geodesy and Geography - Bulgarian Academy of Sciences

This work presents an empirical model for calculating the monthly median values of foE over Bulgaria. The model is based on the regression analysis between the maximum electron density of E-region and the solar zenith angle. The optimal dependence is close to polynomial one. To compare the values of measured monthly median of foE and the same quantity received by the model we presented these two characteristics according to the level of solar activity. Some examples of different years with high and low solar activity reveal that a very good coincidence has been obtained. The mean errors of model for entire interval of almost 20 years are: ME= -0.003 MHz and RMSE=0.083 MHz.

Classification Based on Machine Learning of Fe i 7090A Spectra Derived from CO5BOLD Simulations

Dineva E., Denker C., Verma M., Steffen M., Kontogiannis I.
Leibniz-Institut für Astrophysik Potsdam (AIP)

In the current environment of rapid technological development, data processing and analysis algorithms are required to keep up with the increasingly large and complex observational output. Alongside more-realistic theoretical models, Machine learning (ML) is rapidly integrated into solar and heliophysics research, facilitating analysis of observations and improvement of classical, as well as forward theoretical models. The current project utilizes synthetic spectra of the Fe i 7090.38Å photospheric absorption line, based on CO5BOLD simulations to explore, to explore the potential of Machine Learning algorithms. This specific line was chosen because it is a part of the observing setup for the Fast Multi-line Universal Spectrograph (FaMuLUS) camera system, an instrument currently being commissioned to the Vacuum Tower Telescope (VTT). CO5BOLD snapshots provide a controlled environment, which represents the thermal structure and dynamics of a three-dimensional volume in the solar atmosphere. We developed a pipeline that employs several such algorithms to extract and classify information "hidden" in the large variety of spectral profiles. Using single snapshots as well as time-series gives a more realistic flavor to the simulated observing scenario, where the pipeline will have to deal with, for example, solar feature evolution.

Preliminary Results: Lidar Measurements to Identify Streamers and Analyze Atmospheric Waves LISA (Aeolus+Innovation)

*Kozubek M.², Küchelbacher L.¹, Chum J.², Lastovicka J.², Podolska K.², Sindelarova T.²,
Trinkl F.¹, Wüst S.¹, Bittner M.^{1,3}*

¹German Aerospace Center, DLR-DFD, Oberpfaffenhofen, Germany

²Institute of Atmospheric Physics, CAS-IAP, Prague, Czech Republic

³Institute for Physics, University Augsburg, Augsburg, Germany

Here we present first results within the project LISA. We use Aeolus wind measurements to derivate the planetary wave activity, so-called dynamical activity index (DAI). The DAI represents the mean amplitude of planetary waves up to wavenumber 10 in the mid-latitudes. A comparison of the DAI based on the Aeolus data and ERA-5 reanalysis data is presented. First case studies are shown addressing the structure of streamers and their relation to planetary wave breaking. Due to planetary wave breaking gravity waves might be excited at the flanks of streamers. These flanks are characterized by comparatively strong wind shear. To identify the flanks of the streamer, and so possible source regions for streamers, we calculate the wind gradients along the track. Supplementary measurements are used to further study acoustic GW activity at the ground and at large heights (Doppler sounding or microbarograph measurements). This allows a cross-check of the temporal evolution of the kinetic wave energy density and also provides additional information about the dynamic conditions in the troposphere, stratosphere and mesosphere and give us the general overview of the situation during streamer events. The Aeolus data will be compared with ERA-5 reanalysis data, which provide us the opportunity use reanalysis as an extension in case gaps in observations and because ERA5 provide data every hour we can analyse dynamics continually and independently to observations.

Estimation of the Current Sheet Parameters in Near-Jupiter's Magnetotail Using Simulation

Setsko P.V.¹, Mingalev O.V.^{1,2}, Artemyev A.V.^{3,4}, Melnik M.N.¹

¹Polar Geophysical Institute, Apatity, Russia

²Murmansk Arctic State University, Apatity, Russia

³Space Research Institute, Russian Academy of Science, Moscow, Russia

⁴Department of Earth, Planetary, and Space Sciences, University of California, Los Angeles, USA

Data from Galileo and Juno satellites show that there is a thin current sheet (TCS) in Jupiter's magnetotail, consist of from not only protons, but also hot heavy ions of oxygen O⁺ and sulfur S⁺. The source of these heavy ions is regular volcanic sulfur dioxide emissions from Jupiter's moon Io. For study of transverse spatial scale of this TCS, using numerical model, stationary symmetric configurations for several variants of counter longitudinal ions flows forming TCS were obtained. From calculation results, we can say the following:

- If CS is formed only by flows of hot sulfur ions, then it has the largest half-width $L \sim 0.27-0.32R_J \sim 3-3.5R_E$, as well as the smallest maximum values of the current density and concentration in the center of CS $J_{Smax} \sim 1.5nA/m$ and $n_{Smax} \sim 0.024 sm^{-3}$
- If CS is formed only by flows of hot oxygen ions, then it has a smaller half-width $L \sim 0.22R_J \sim 2.5R_E$ and values of the current density and concentration in the center of CS two times bigger than for first case $J_{Omax} \sim 3nA/m$ and $n_{Omax} \sim 0.048 sm^{-3}$
- If CS is formed only by flows of protons, then it has the smallest half-width $L \sim 0.036 R_J \sim 0.4 R_E$, as well as the biggest maximum values of the current density and concentration in the center of CS $J_{Pmax} \sim 16nA/m$ and $n_{Pmax} \sim 0.095 sm^{-3}$, comparable with Earth's TCS.

So, compare our results with satellite date we can conclude that hot sulfur ions made main contribution to the total current through the CS in the near-Jupiter's magnetotail.

Instrumentation for Space Weather Monitoring

Overview about VIRAC and Ongoing Activities

Bezrukovs V., Klokovs A.

Ventspils International Radio Astronomy Centre (VIRAC) of Ventspils University of Applied Sciences (VUAS)

Ventspils International Radio Astronomy Centre (VIRAC) of Ventspils University of Applied Sciences (VUAS) was established in 1994 with the aim to develop the research activities in radio astronomy, astrophysics and space sciences. The most important instrumental base for the centre comprised two fully steerable parabolic antennas, RT-16 and RT-32 (i.e., with the mirror diameter of 16 m and 32 m) and LOFAR-LATVIA station. The intensive reconstruction and instrumental refurbishment carried out in 2014 – 2019 made it possible to use radio telescopes for the international scale fundamental and applied research in the field of radio astronomy. The most important aspect of this work is participation in the VLBI (Very Long Baseline Interferometry) international experiments. During the renovation, radio telescopes were instrumented with two channel right circular polarization (RCP) and left circular polarization (LCP) cryogenic broad band receivers with frequency coverage of 4.5 – 8.8 GHz and instantaneous bandwidth of approx 1200 MHz.

Overview of the Space Radiation Extreme Events Observed with Liulin Type Instruments

*Dachev T.¹, Tomov B.¹, Matviichuk Y.¹, Dimitrov P.¹, Semkova J.¹, Koleva R.¹,
Jordanova M.¹, Bankov N.¹, Mitev M.¹, Krastev K.¹, Malchev S.¹, Mitrofanov I.², Litvak
M.², Kozyrev A.², Golovin D.², Reitz G.³, Header D.-P.⁴, Benghin V.⁵, Shurshakov, V.⁵*

¹SRTI-BAS, Sofia, Bulgaria

²SRI-RAS, Moscow, Russia

³DLR, Köln, Germany

⁴Möhrendorf, Germany

⁵IBMP, Moscow, Russia

The paper presents the space radiation extreme events observed with Liulin type instruments. The following events were classified as extreme: solar energetic particles (SEP), relativistic electron enhancements (REE) and burst type REE. We compare the dose rates and flux data from 5 SEP events in 1989, 2012, 2015, 2021 and 2022, 2 REE events in 2010 and 2015 and 1 burst type REE in 2015. The dose rates and flux data, measured in the inner and the outer radiation belt maxima at 3,000 and 20,000 km, respectively, registered by RADOM instrument in 2008, are compared with the extreme events data. The Liulin experiments names used are LIULIN, Liulin-5, Liulin-MO, RADOM, R3DR1 and R3DR2. All data were selected to cover periods of about 6 hours and 30 minutes that are the average continuation of the extravehicle activities on the ISS. The time intervals were chosen to coincide with the maximum of the observed dose rates and fluxes during different events.

Acknowledgements. The work in Bulgaria is supported by grant KP-06 Russia 24 for bilateral projects of the National Science Fund of Bulgaria and Russian Foundation for Basic Research.

Solar Influences on the Lower Atmosphere and Climate

Solar Influence on Ozone Variations over ENSO Regions

Chapanov Y.

Climate, Atmosphere and Water Research Institute, Bulgarian Academy of Sciences

The most important source of ENSO excitation is the influence of harmonics of solar activity cycles. The solar activity is revealing mainly by the Total Solar Irradiance (TSI) variations, solar wind and variations of solar magnetic field. While the TSI variations affect directly earth surface temperature, the solar wind and magnetic field modulate changes of the heliosphere, geomagnetic field and cosmic ray variations. The cosmic ray variations drive ozone production in low stratosphere near the tropopause, and next a chain process affects surface temperature. These effects are proved in polar and ENSO regions. In previous studies, a strong correlation has been found between ozone and El Nino variations; and between the variations of indices of N-S solar asymmetry and Nino 3.4. So, the possible transmitter between solar signals and ENSO event is low stratosphere ozone, whose variations are affected by solar activity. The solar influence on ozone variations over ENSO regions is investigated by means of time series of solar activity indices and ozone variations at 70 hPa over some ENSO regions around equatorial part of Pacific Ocean. The common harmonics of solar and ozone cycles are determined by means of recently developed Method of Partial Fourier Approximation, where the trigonometric coefficients are estimated by the Method of Least Squares. The results of common frequency bands with interannual, decadal and centennial periodicity of solar and ozone data may improve models of solar influence on Pacific temperature anomalies and recent climate change.

Space Weather Effects on the Atmosphere

Georgieva K., Kirov B.

SRTI-BAS

A number of solar activity manifestations can affect the Earth's atmosphere. The total solar irradiance is the main energy source for the terrestrial system. Radiation in different spectral ranges affects different parts of the Earth's atmosphere. With decreasing wavelength, the relative variations increase.

The Earth is also exposed to the flow of charged particles with embedded magnetic fields from the solar corona (the solar wind). On top of it, transient structures like Coronal Mass Ejections (CMEs) and High Speed Solar Wind Streams (HSSs) ride whose interactions with the geomagnetic field lead to geomagnetic storms.

High energy particles from CME or HSS associated shocks, or from the magnetosphere, precipitate in the high latitude atmosphere leading to increased ionization, enhanced production of compounds which affect the ozone balance, radiative heating and cooling, and finally changes in atmospheric dynamics and large-scale circulation modes like the North Atlantic Oscillation governing the weather over most of the Northern hemisphere.

The solar wind magnetic field modulates the flux of galactic cosmic rays, high energy particles coming from outside the Solar system which penetrate deep into the atmosphere. Their variations are found to be strongly correlated with the atmospheric global electric circuit, cloud cover, albedo, and infrared opacity, determining the Earth's energy balance.

In this review We will describe its above mentioned agents, and explain the suggested mechanisms by which they influence the atmosphere and climate. We will present observational evidences of such influences, highlight the recent advances, and the still unsolved questions and uncertainties.

Colours of the Eclipsed Moon - Effects of Stratospheric Transparency and Solar Activity

Gospodinov D.

Space Research and Technology Institute – Bulgarian Academy of Sciences, Stara Zagora Department

Solar activity influence on the colour of the moon during total lunar eclipses is considered in the work.

The umbra is always sufficiently dark to the naked eye, the fully eclipsed part of the lunar disk appears almost black in contrast to the uneclipsed portion. Only in a total lunar eclipse, during the phase of totality itself, can the color of the illuminated disk become a reliable indicator of stratospheric turbidity.

Colors other than red can also appear during a total lunar eclipse, especially near the moon's rim. Although this fact has been known since ancient times, modern methods of reporting eclipse colors have ranged from traditional, simple visual descriptions to more objective photometric measurements.

Catalogue of the observed colors during the 1960–2020 period has been made in the Yuri Gagarin Public Astronomical Observatory and Planetarium, Stara Zagora. Usable eclipses' number is 42. The hue and intensity of the faint illumination of the lunar disk during totality yield a measure of the aerosol optical depth of the Earth's stratosphere. This period under study showed a relatively clear stratosphere at nearly all times.

Physical phenomena in the earth's atmosphere, which have an effect on the earth's umbra structure are discussed. Heterogeneous colour of the moon during a total eclipse is connected with stratospheric structures of different physical state.

Good correlation between the solar indices and colour of the eclipsed Moon, estimated by the Danjon scale serve as a proof of the solar activity and stratospheric phenomena connection.

The Statistical Analysis of Air Crash Investigations from 1918 to 2022 and Comparison with Geomagnetic Storms

Göker Ü.D.¹, Kobanoğlu B.², Akçay Ç.³, İpek M.⁴, Eratılmış M.⁵

¹Istanbul Ayvansaray (Topkapı) University, Faculty of Economics, Administrative and Social Sciences, Department of Aviation Management;

²Istanbul Ayvansaray (Topkapı) University, Institute of Graduate Studies, Management Information Systems;

³National Defense University, Air Force Academy, Department of Aviation and Space Engineering;

⁴National Defense University, Air Force Academy, Department of Aviation and Space Engineering;

⁵Istanbul Ayvansaray (Topkapı) University, Institute of Graduate Studies, Management Information Systems

Air transportation is one of the most preferred types of transportation for many reasons. However, to minimize the risk of accidents with developing technology, investigations and studies are carried out by many organizations. While the main causes of accidents in the first years of aviation were due to mechanical reasons, accidents caused by mechanical reasons have been replaced by an increase in the number of aircraft accidents caused by human-induced errors which depend on the increasing manpower with the developing technology. In addition to these, meteorological accidents have an important place in our list because there are no survivors in accidents caused by meteorological events. More importantly, it is often not possible to predict meteorological accidents. However, apart from the accidents whose causes have been explained, the percentage of the accidents that have not been found so far is also very high. In this talk, all these reasons which cause air crashes are mentioned and the statistical analysis of air crashes between the years 1918-2022 is examined. Finally, the correlation of all these accidents with geomagnetic storms is calculated. This study has changed our perspective on the cause of many unexplained air crashes or the occurrence of many accidents without consideration of geomagnetic storms.

Space weather and its effects on spacecraft charging

Kirov B., Georgieva K., Asenovski S.

Space Research and Technology Institute, Bulgarian Academy of Sciences

In the current work we describe the Langmuir Probe (LP) and its operation on board the International Space Station. This instrument is a part of the scientific complex “Ostonovka”. The main goal of the complex is to establish, on one hand how such big body as the International Space Station affects the ambient plasma and on the other how Space Weather factors influence the Station. The LP was designed and developed at BAS–SRTI.

Digitization of Meteorological Data Archives Collected in Bulgaria

Shirov G., Petrov N., Tsvetkov Ts.

Institute of Astronomy and National Astronomical Observatory, Bulgarian Academy of Sciences

We use the data archive of National Institute of Meteorology and Hydrology to analyse climate changes in Bulgaria in the last more than 100 years. First step of our task is to digitalize the data collected since 1906. The archive includes monthly mean numerical data of selected weather elements, i.e. temperature, rainfall amount, wind speed and direction, atmospheric pressure. Our goal is to create a database documenting meteorological measurements and to check for a possible solar influence on observed variations.

Peculiar Atmospheric Electric Field Response at High Latitude to Three Major SEP Events in 2001 and Its Possible Interpretation

Tonev P.

SRTI-BAS

We analyse here the results from measurements of the atmospheric electric field E_z variations at ground level obtained at the high-latitude observatory in Apatity (geomagnetic latitude 63.8) during three major solar proton events (SPE) with GLE in 2001 (on 15.04, 18.04, and 04.11, respectively), and propose hypothetical interpretation. For each of these SPE E_z demonstrates extremely large and peculiar variations in two separate time periods: a) throughout the SPE, and b) well before the SPE and its causative solar flare. This type of E_z behavior cannot be explained in terms of classical theory of the global atmospheric electrical circuit. To interpret the peculiar E_z variations during SPE we proposed earlier a hypothetical principal explanation based on assumption for creation of aerosol layers contributing to modifications of the atmospheric conductivity profile. In order to explain the E_z behavior observed before each SPE, several factors are involved including the observed significant X-ray enhancements which can affect the ionization rate and conductivity in middle atmosphere.

Long-Term Variability of North Atlantic Cyclone Tracks: Possible Influence of Solar Activity and Galactic Cosmic Rays

Veretenenko S., Dmitriev P.
Ioffe Institute RAS, St. Petersburg, Russia

In this work we study long-term changes of extratropical cyclone tracks in the North Atlantic in cold months (October-March) basing on Mean Sea Level Pressure archives from Climatic Research Unit, UK (1873-2000) and NCEP/DOE AMIP-II Reanalysis (1979-2021). It was revealed that trajectories of North Atlantic cyclones are characterized by noticeable variability on bidecadal, multidecadal and secular time scales, which may be associated with solar activity and related phenomena. Cyclone tracks were found to shift a few degrees south at the maximum of the secular Gleissberg cycle, whereas at the minimum and the declining phase of the cycle they shift to the north. Another distinguished feature of North Atlantic cyclone tracks is roughly 22-year oscillations, which are close to the magnetic Hale cycle on the Sun. A possible mechanism of solar activity effects on cyclone movement may involve changes in the strength of the stratospheric polar vortex due to ionization changes caused by auroral electrons and galactic cosmic rays.

Wavelet Analysis and Recurrence Plots of Oxygen Isotope and Paleotemperature Records from NGRIP Ice Core

Wysokinski A., Kobylnski Z.
¹Independent researcher, Iganie, Poland
²High School of National Economics, Kutno, Poland

High resolution climate records of the oxygen 18 in the ice core with 50 yr sampling averages obtained by North Greenland Ice Core Project, which extends now back to more than 150000 years before the present and available from World Data Center for Paleoclimatology. They are studied by means of recurrence plots and wavelet technique with established significance levels. Both methods go to make the suitable tool to derive spectral information of the data both as a function of frequency or wavelength and time. The records are compared also with measurements from Antarctica. The obtained results indicates that the stronger variability of the oxygen 18 content are related to cooler, glacial seasons. The paper is an extension of earlier presented poster at Peking COSPAR meeting.

Solar Effects in the Biosphere and Lithosphere

Assessment of the Space Weather Hazard over Romanian Territory

Dobrica V.¹, Demetrescu C.¹, Isac A.², Stefan C.¹

¹Institute of Geodynamics, Romanian Academy

²Geological Institute of Romania

The space weather hazard from geomagnetically induced currents (GICs), known to affect the technological systems during certain space weather events that produced large geomagnetic storms, is investigated over the Romanian territory via the surface geoelectric field. The surface electric field, induced by the variable magnetic field of geomagnetic storms, is determined based on the geomagnetic field recordings from the Surlari geomagnetic observatory and on information regarding the underground electric conductivity from a recent magnetotelluric model of the Romanian lithosphere. The surface geoelectric field associated to geomagnetic variations during major geomagnetic storms of the solar cycle 23 (1986-1996) ($Dst < -150$ nT) is determined using the plane wave approximation for the depth propagation of the geomagnetic disturbance.